Stationary Spatially Complex Solutions in Cross-Flow Reactors with Two Reactions

Moshe Sheintuch and Olga Nekhamkina
Dept. of Chemical Engineering, Technion—I.I.T., Technion City, Haifa 32 000, Israel

Formation of stationary spatially multiperiodic or even chaotic patterns is analyzed for a simple model of a cross-flow reactor with two consecutive reactions and realistically high Le and Pe. Spatial patterns emerge much like dynamic temporal patterns in a mixed system of the same kinetics. The sequence of period doubling bifurcations is determined for the corresponding ODE system and is completely confirmed by direct numerical simulations of the full PDE model. The incorporation of a slow nondiffusing inhibitor led to chaotic spatiotemporal patterns.

Introduction

In this work we construct stationary spatially complex patterns in cross-flow reactors. The idea conveyed here is at the crossroads of two concepts: patterns in cross-flow reactors and chaotic solutions. Cross-flow reactors, in which most of the feed is distributed along the reactor, can attain, under certain assumptions and far from the inlet, a homogeneous (space-independent) solution. This can be advantageous in an operation in which we want to maintain a reactor at a fixed temperature and concentration due to selectivity considerations or due to self-inhibitory kinetics. The unique aspect of such a reactor, with a single exothermic reaction, is that it can attain a stationary spatially periodic solution (Nekhamkina et al., 2000b, 2001). Such a reactor model will typically be (under the assumptions outlined later) of the form

$$LeT_t - T_{zz}/Pe + T_z = f(T, C), \qquad C_t + C_z = g(T, C) \quad (1)$$

Noticing that $T_t = f$, $C_t = g$ is the system describing the dynamics of a homogeneous CSTR (that is, with no solid heat capacity) of similar kinetics, we explained in earlier works how the temporal behavior in a CSTR is translated into a spatial behavior in a cross-flow reactor of high *Pe* and high *Le* numbers (which are typically the characteristics of commercial reactors) and subject to Danckwerts boundary conditions at the reactor inlet. This mechanism is a novel approach for establishing stationary spatially periodic patterns and is different from the Turing mechanism (Turing, 1952) which applies to a two-variable system when the inhibitor (C, in our case) diffuses sufficiently faster than the activator (T) and which is widely employed in reaction–diffusion systems (Murray, 1993; De Wit, 1999).

Formation of stationary spatially periodic patterns in convective–reaction–diffusion systems due to this novel mechanism does not depend on the ratio of diffusivities (actually the inhibitor may be nondiffusing). This mechanism can be viewed as the amplification effect of the stationary perturbations, which are introduced into the system by the boundary conditions (BC). The structure of regular patterns, however, does not depend on the BC, which affect solutions in the entrance zone only. Other studies of convection–reaction–diffusion systems predicted stationary solutions using the Brusselator model (Kuznetsov et al., 1997; Andresén et al., 1999), the Gray–Scott kinetics (Satnoianu and Menzinger, 2000; Satnoianu et al., 2001), the CDIMA reaction and the Oregonator model (Bamforth et al., 2000, 2001).

In our previous works we studied a cross-flow reactor with a single first-order Arrhenius kinetics (Nekhamkina et al., 2000a,b, 2001). In this article we extend the analogy to systems of two reactions, showing that with two consecutive reactions and using parameters that admit temporally chaotic solutions in a CSTR, we can find stationary spatially complex solutions in a cross-flow reactor. Moreover, the bifurcation scenario leading to temporal chaos is also the scenario leading to spatial complexity. For the example studied here, the corresponding CSTR system exhibits a sequence of period-doubling bifurcations with a varying parameter (say p) at $p = p_1, p_2, \ldots, p_n$. Then, for the spatially distributed system with $p = p_n$ and other fixed parameters we can expect to find a

Correspondence concerning this article should be addressed to M. Sheintuch.

spatially 2^n-periodic solution in the limiting case, $Pe \to \infty$. With increasing Pe, the bifurcation from a homogeneous to periodic solutions is always via a period-one solution at some critical $Pe = Pe_0$, which can be determined from linear analysis (see, for example, Nekhamkina et al., 2000). For finite $Pe > Pe_0$, we expect to find, as we increase Pe to ∞, a sequence of bifurcations leading to formation of the $2n$ spatially periodic solution. Note, that this scenario is not evident *a priori*, because the stationary patterns in the distributed system do not necessarily have to be sustained.

Since chaos requires an infinitely long time or space, we cannot claim that we achieve spatial chaos, but we can get as close as necessary with a sufficiently long reactor. Temporal chaos has been a subject of extensive investigation of CSTR models with two consecutive reactions (Lynch et al., 1982; Lynch, 1992; Jorgensen and Aris, 1983; Jorgensen et al., 1984; Doedel and Heinemann, 1983; Chembukar et al., 1987; Abashar and Elnashaie, 1997, among others). Once we understand the translation mechanism of the temporally periodic solutions into spatially periodic states in cross-flow reactors, we can argue that a similar outcome is expected in other situations that admit temporal chaos, such as two parallel reactions (see Chan et al., 1987), reactions with complex kinetics, or a periodically forced oscillator; the latter should be translated to a system with spatially periodic properties (such as the heat-transfer coefficient) in the cross-flow reactor.

Other phenomena that are expected in a system with two reactions, such as tristability (three stable solutions out of a possible five) of homogeneous solutions, and the possibility of producing moving fronts that separate various combinations of states, are not discussed here.

Note that a thermokinetic model like Eq. 1 cannot predict temporal oscillations in a catalytic mixed reactor ($LeT_t = f$, $C_t = g$), due to its high heat capacity, and cannot serve as a model for catalytic oscillators. Catalytic oscillators usually incorporate a slow localized inhibitor that can induce moving or oscillatory patterns. We also consider the incorporation of such a step to find out whether the complex stationary solutions will undergo a bifurcation to oscillatory patterns that may be chaotic in time and in space (that is, turbulent).

The results presented here should be also mapped within the wide domain of instabilities in packed-bed systems. Sustained stationary fronts or spatiotemporal patterns in regular packed beds (that is, as opposed to crossflow) can result from the interaction of heat and mass balances, which typically produce moving fronts for positive-order kinetics (Frank-Kamenetsky, 1955; Zeldovich and Barenblatt, 1959; Puszynski et al., 1981; also, see the review by Merzhanov and Rumanov, 1999), patterns with oscillatory kinetics (see the review by Sheintuch and Shvartsman, 1996; Sheintuch and Nekhamkina, 1999a,b), or with feedback loops (Hua et al., 1994; Berezowski et al., 2000). These mechanisms do not predict stationary spatial patterns.

Extensive studies into patterns in convection–diffusion–reaction systems, of the type that can exhibit homogeneous solutions due to cross-flow feeding or due to consecutive reactions, demonstrated that patterns may emerge with two reactants that flow at different convective rates because of the differential flow-induced chemical-instability (DIFICI) mechanism (Rovinsky and Menzinger, 1992; Yakhnin et al., 1994). Physically, flow differentiation cannot apply to simple fixed beds, but can apply to the motion of ions due to a potential field. The equations describing such a system can be converted to a form similar to ours, as we will discuss elsewhere. Yet, the DIFICI mechanism was shown to account for spatiotemporal patterns, while we demonstrate the existence of stationary patterns.

We should emphasize again that we are not aware of any demonstration of stationary spatially complex patterns in any convection–diffusion–reaction system.

The structure of this work is as follows: in the next section the mathematical model is formulated, linear analysis and bifurcation diagrams are presented in the third section, and in the fourth one numerical simulations with analytical predictions are compared.

Mathematical Model

We employ a homogeneous one-dimensional (1-D) model of a catalytic cross-flow reactor, in which two consecutive reactions, $A \to B \to C$, take place. Interphase gradients of temperature and concentrations between the fluid and solid phases are assumed to be negligible. The mass and energy balances account for accumulation, convection, axial dispersion, chemical reactions $r_i(C_A, C_B, T, \phi)$, heat loss due to cooling $[(S_T = h_T P(T - T_w)]$ and mass supply through a membrane wall ($S_{C_A} = k_g P(C_A - C_{Aw})$, $S_{C_B} = k_g P(C_B - C_{Bw})$; the source terms are assumed to follow simple gradient law, where C_{Aw} and C_{Bw} are assumed to be constants and the mass supply is assumed not to significantly affect the molar flow in the reactor)

$$\frac{\partial C_A}{\partial t} + u\frac{\partial C_A}{\partial z} - \epsilon D_{fA}\frac{\partial^2 C_A}{\partial z^2} = -(1-\epsilon)r_1(C_A, T, \phi) + S_{C_A}$$

$$\frac{\partial C_B}{\partial t} + u\frac{\partial C_B}{\partial z} - \epsilon D_{fB}\frac{\partial^2 C_B}{\partial z^2} = (1-\epsilon)r_1(C_A, T\,\phi) - (1-\epsilon)r_2(C_B, T, \phi) + S_{C_B}$$

$$(\rho c_p)_e\frac{\partial T}{\partial t} + (\rho c_p)_f u\frac{\partial T}{\partial z} - k_e\frac{\partial^2 T}{\partial z^2} = (1-\epsilon)(-\Delta H_1)r_1 \times (C_A, T, \phi) + (-\Delta H_2)r_2(C_B, T, \phi)) + S_T \quad (2)$$

We use conventional notation: u is the molar velocity, so that the change is negligible for dilute reactants; $C_i (i = A, B)$ is the reactant mole fraction; ϵ is the bed void fraction; the subscripts f and e denote the fluid phase, and an efficient value (a weighted average value of the corresponding fluid and solid phase properties), respectively. The Danckwerts boundary conditions are typically imposed on the system

$$z = 0: \quad \epsilon D_{fA}\frac{\partial C_A}{\partial z} = u(C_A - C_{A,in})$$

$$\epsilon D_{fB}\frac{\partial C_B}{\partial z}u(C_B - C_{B,in}), \qquad k_e\frac{\partial T}{\partial z} = (\rho c_p)_f u(T - T_{in})$$

$$z = L: \quad \frac{\partial T}{\partial z} = \frac{\partial C_A}{\partial z} = \frac{\partial C_B}{\partial z} = 0 \quad (3)$$

We assume that the dispersion of mass is negligible. For a first-order activated kinetics with a rate that is proportional to the catalytic activity (ϕ), that is, $r_i(C_i, T, \phi) = A_i \phi C_i \exp(-E_i/RT)$, the system (Eqs. 2 and 3) can be rewritten in the dimensionless form as

$$\frac{\partial x_1}{\partial \tau} + \frac{\partial x_1}{\partial \xi} = -\bar{r}_1(x_1, y, \phi) - \alpha_C(x_1 - x_{1,w}) = f(x_1, y, \phi)$$

$$\frac{\partial x_2}{\partial \tau} + \frac{\partial x_2}{\partial \xi} = \bar{r}_1(x_1, y, \phi) + \bar{r}_2(x_2, y, \phi) - \alpha_C(x_2 - x_{2,w}) = g(x_1, x_2, y, \phi)$$

$$Le\frac{\partial y}{\partial \tau} + \frac{\partial y}{\partial \xi} - \frac{1}{Pe}\frac{\partial^2 y}{\partial \xi^2} = B(\bar{r}_1(x_1, y, \phi) + \sigma \bar{r}_2(x_2, y, \phi)) - \alpha_T y = h(x_1, x_2, y, \phi); \quad (4)$$

$$\xi = 0, \qquad x_1 = x_{1,in}, \qquad x_2 = x_{2,in}, \qquad \frac{1}{Pe}\frac{\partial y}{\partial \xi} = y;$$

$$\xi = \tilde{L}, \ \frac{\partial y}{\partial \xi} = 0 \quad (5)$$

Here conventional notation is used

$$x_1 = \frac{C_A}{C_{A,w}}, \qquad x_2 = \frac{C_B}{C_{A,w}}, \qquad y = \gamma\frac{T - T_w}{T_w}, \qquad \xi = \frac{z}{z_0}$$

$$\tau = \frac{tu}{z_0},$$

$$\bar{r}_1(x_1, y, \phi) = -Da_1 \phi x_1 \exp\left(\frac{\gamma y}{\gamma + y}\right)$$

$$\bar{r}_2(x_2, y, \phi) = Da_1 \phi \nu x_2 \exp\left(\frac{\lambda \gamma y}{\gamma + y}\right)$$

$$\gamma = \frac{E_1}{RT_w}, \qquad B = \gamma\frac{(-\Delta H_1)C_{A,w}}{(\rho c_p)_f T_w}$$

$$Da_1 = \frac{A_1(1-\epsilon)z_0}{u}e^{-\gamma}$$

$$\nu = A_2/A_1 \exp(E_1 - E_2)/RT_w, \qquad \sigma = \frac{\Delta H_1}{\Delta H_2}, \qquad \lambda = \frac{E_2}{E_1}$$

$$Le = \frac{(\rho c_p)_e}{(\rho c_p)_f}, \qquad Pe = \frac{(\rho c_p)_f z_0 u}{k_e}, \qquad \alpha_C = \frac{k_g P z_0}{u}$$

$$\alpha_T = \frac{h_T P z_0}{(\rho c_p)_f u} \quad (6)$$

Note that we use an arbitrary value for the length scale (z_0), so that the reactor length $\tilde{L} = L/z_0$ can be varied as a free parameter. The conventional definition of Peclet corresponds to ours as $Pe\tilde{L}$.

As stated earlier we initially set the activity to be constant ($\phi = 1$). We consider the effect of varying ϕ later. While there is no general agreement on the source and rates of activation/deactivation, here we adopt a simple linear expression (see Barto and Sheintuch, 1994) that assumes that deactivation occurs faster at higher temperatures and at higher activities and that its rate is independent of reactant concentration. Thus, the dimensionless form of the catalytic activity variation is

$$K_\phi \frac{d\phi}{d\tau} = a_\phi - b_\phi \phi - y = q(y, \phi) \quad (7)$$

and typically $K_\phi \gg 1$. Recall that the time scale of autocatalytic thermal changes is Le, and changes of activity of a similar magnitude to Le or larger will be significant when K_ϕ.

The solutions of the righthand side of the system (Eqs. 4 and 7), that is, $f(x_{1,s}, x_{2,s}, y_s, \phi_s) = g(x_{1,s}, x_{2,s}, y_s, \phi_s) = h(x_{1,s}, x_{2,s}, y_s, \phi_s) = q(y_s, \phi_s) = 0$, are the asymptotic homogeneous solutions of the distributed problem. For regular kinetics ($\phi = 1$), up to five solutions can exist within a certain set of parameters (Jorgensen et al., 1984); for the case of varying catalytic activity, the problem of multiplicity of the steady-state solutions is beyond the scope of this study.

Bifurcation Analysis

Constant activity case: $\phi = 1$

To understand the patterns admitted by the system (Eqs. 4) it is pertinent to recall the analogy between the stationary solutions of the cross-flow reactor, and the temporal behavior of the CSTR lumped system (see our previous works, Nekhamkina et al., 2000a,b, 2001).

We, therefore, analyze several simplified and related systems:

1. If we ignore the heat-dispersion term, then the steady-state model of the distributed system

$$\frac{dx_1}{d\xi} = f(x_1, y, 1) = f_1(x_1, y)$$

$$\frac{dx_2}{d\xi} = g(x_1, x_2, y, 1) = g_1(x_1, x_2, y)$$

$$\frac{dy}{d\xi} = h(x_1, x_2, y, 1) = h_1(x_1, x_2, y) \quad (8)$$

is exactly the model describing the temporal dynamics of a homogeneous CSTR with two consecutive reactions (with ξ replaced by time). This problem has been investigated extensively for the case of the constant catalytic activity in order to map the various bifurcation diagrams and phase planes in the parameter space (Jorgensen et al., 1984; Chemburkar et al., 1987; Abashar et al., 1997; among others).

2. Incorporating the dispersion term now, while still maintaining the steady state, the system is described by

$$\frac{dx_1}{d\xi} = f_1(x_1, y); \qquad \frac{dx_2}{d\xi} = g_1(x_1, x_2, y); \qquad \frac{dy}{d\xi} = p;$$

$$\frac{dp}{d\xi} = Pe[p - h_1(x_1, x_2, y)] \quad (9)$$

The solutions of this system are identical to that of Eq. 8 in the limiting case, $Pe \to \infty$, but for finite Pe the system (Eq. 9) may possess additional solutions. The critical Pe_0 that marks

the bifurcation to a spatially periodic solution (corresponds to a Hopf bifurcation) can be determined from linear stability analysis.

3. We can conduct a linear stability analysis of the full system (Eq. 4) in an infinitely long region, which is not affected by the boundaries. Denoting a small deviation from the basic steady-state solution $\boldsymbol{u}_0 = \{x_{1s},\ x_{2s},\ y_s\}$ as $\boldsymbol{u}_1 = \{x_1,\ x_2,\ y_1\}$, we arrive at the following linearized system for the perturbations

$$\boldsymbol{A}\frac{\partial \boldsymbol{u}_1}{\partial \tau} - \frac{\partial \boldsymbol{u}_1}{\partial \xi} - \boldsymbol{D}\frac{\partial^2 \boldsymbol{u}_1}{\partial \xi^2} = \boldsymbol{J}\boldsymbol{u}_1 \tag{10}$$

where $\boldsymbol{A} = \mathrm{diag}\{0,\ 0,\ Le\}$ and $\boldsymbol{D} = \mathrm{diag}\{0,\ 0,\ (Pe)^{-1}\}$ are the capacity and diffusivity matrices, and $\boldsymbol{J}$, with elements $\{j_{mn}\}$, is the Jacobian matrix of the linearized system (Eq. 4) evaluated at the steady state (with $\phi = 1$). We seek a solution of Eq. 10 in the form of the normal modes

$$\boldsymbol{u}_1 = \boldsymbol{U}_0 e^{ik\xi + \sigma\tau} \tag{11}$$

where $\boldsymbol{U}_0$ is a constant vector, k is the perturbation wave number, and σ is the time growth rate. Substituting Eq. 11 into Eq. 10, we obtain the *dispersion relation*

$$\mathfrak{D}(\sigma, k) = Le\sigma^3 + D_2(k)\sigma^2 + D_1(k)\sigma + D_0(k) = 0 \tag{12}$$

where the coefficients $D_i(k)$ are

$$D_0(k) = k^2 Tr + \frac{k^2}{Pe}\left(M_{12} - k^2\right) - \Delta + ik\left[S_M - k^2 - \frac{k^2}{Pe}(j_{11} + j_{22})\right]$$

$$D_1(k) = M_{13} + M_{23} - 2k^2 + Le\left(j_{11}j_{22} + j_{12}j_{21} - k^2\right) - \frac{k^2}{Pe}(j_{11} + j_{22}) - ik\left[(j_{11} + j_{22})(Le + 1) + 2j_{33} - \frac{k^2}{Pe}\right]$$

$$D_2(k) = \frac{k^2}{Pe} - j_{33} - Le(j_{11} + j_{22}) + ik(1 + 2Le) \tag{13}$$

Here

$$Tr = Tr[\boldsymbol{J}], \qquad \Delta = det[\boldsymbol{J}],$$

$$M_{mn} = j_{mm}j_{nn} - j_{mn}j_{nm}, \qquad m, n = 1, 2, 3;$$

$$S_M = M_{12} + M_{13} + M_{23}$$

The bifurcation condition $Re\ \sigma = 0$ defines the neutral curve, which can be calculated numerically for a chosen set of parameters. We use Pe as the bifurcation parameter, since we intend to employ the similarity between the stationary patterns emerging at $Pe \to \infty$ for Eq. 4 and the dynamic behavior of the corresponding CSTR problem. The neutral curve typically acquires a minimum (k_c, Pe_c; see Figure 1), and crossing Pe_c, excites, in an unbounded system, a wave packet with finite k moving at a constant speed.

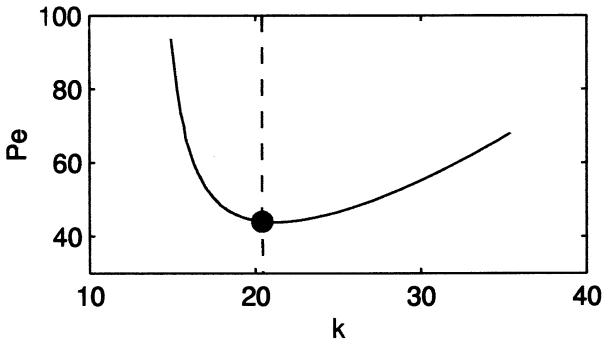

Figure 1. Typical neutral curve defined by $Re\,\sigma = 0$ (solid line) for the constant activity case, $Im\,\sigma = 0$ (dashed line).

The dot denotes the critical point Pe_0, k_0 defined by Eq. 14. Other parameters: $Da_1 = 0.26$, $Da_2 = 0.13$, $B_1 = 57.77$, $B_2 = -24.61$, as in Chemburkar et al. (1987), $\alpha_T = 8.94$.

4. Let us consider now the bounded system governed by Eq. 4 and subject to the stationary boundary conditions (Eq. 5). As was demonstrated previously (Nekhamkina et al., 2000a), the moving patterns predicted to exist in an infinite region are arrested by the boundaries, and above some threshold are transformed into *stationary patterns*. These generally do not correspond to the minimum of the neutral curve, and for such patterns to emerge, we have to impose a condition of zero phase velocity (or zero frequency $\omega = Im\,\sigma = 0$) in addition to the relation $Re\,\sigma = 0$. This second condition also defines a curve in the plane (Pe, k) that may be calculated numerically (see Figure 1). At the intersection of these conditions we can determine the critical point—a threshold value for amplification of stationary perturbations. The critical parameters can be derived from the bifurcation condition (Eq. 12), which, for $\sigma = 0$, is reduced to the relation $D_0(k) = 0$. Separating the real and imaginary parts of D_0, we obtain the following equations for the critical Pe_0 and k_0

$$\frac{k_0^2}{Pe_0} = \frac{S_M - k_0^2}{j_{11} + j_{22}}; \qquad \left(k_0^2 - M_{12}\right)\frac{k_0^2}{Pe_0} - k_0^2 Tr + \Delta = 0 \tag{14}$$

Note that Pe_0 and k_0 defined by Eq. 14 correspond to the Hopf bifurcation point of the ODE system (Eq. 9), but k_0 is now the spatial wave number. We do not attempt to plot the domain of parameters where oscillatory solutions exist.

Before starting the next step of the analysis, recall that we want to inquire whether the stationary spatially multiperiodic or even chaotic patterns can be sustained in the system. In order to simplify the analysis (the search of the parameter space), we employed the well-known results obtained for the lumped CSTR model. As was mentioned earlier, each type of periodic or even chaotic temporal behavior in the CSTR model can be formally considered to be a limit of the corresponding stationary solutions of the distributed system for $Pe \to \infty$. We can reasonably assume that this multiperiodic solution can, in turn, be obtained as a sequence of bifurcations with increasing Pe, from Pe_0 to ∞. We search for a set of

parameters that admits multiperiodic or chaotic solutions in a relatively wide range of the bifurcation parameter, and possesses critical parameters (Pe_0) and spatial wave length ($T_1 = 2\pi/k_0$) that allows observations of these motions in a distributed system with a physically reasonable reactor length (L) and Peclet (Pe) values (see discussion below). In the first study of chaos due to two consecutive reactions (Jorgensen and Aris, 1983), the domain of the multiperiodic and chaotic solutions is extremely small (transition from the period-two solution to chaos occurs by increasing a heat transfer coefficient from 7.28295 to 7.28667, while the periods of oscillations are sufficiently large ($T_1 \sim 1.73$)). In another work, for example, by Abashar and Elnashaie (1997), for a similar lumped model the period adding bifurcations was obtained in a relatively large range of the gain coefficient K (an analog of the heat-transfer coefficient); however, the period of oscillations is extremely large ($T_1 \sim 40$).

For our study we chose the set of parameters employed in a CSTR by Chemburkar et al. (1987) for exothermic–endothermic consecutive reactions. According to the bifurcation diagram obtained in this work using the heat transfer coefficient δ (notation used by Chemburkar et al., 1987) as the bifurcation parameter, the steady-state solution of the CSTR model loses stability via a Hopf bifurcation at $\delta = 6.9408$ with $T_1 = 0.371$. The following increase in δ led to a sequence of period-doubling bifurcations that converges to chaotic solutions that exist at $7.965 < \delta < 8.04125$. (To be consistent with that study, we set $\alpha_T = \delta + 1$, $x_{1,w} = 1$, $x_{2,w} = 0$, $y_w = 0$.)

We constructed the bifurcation diagrams of the ODE system (Eq. 9) using Pe as a bifurcation parameter for the set of the parameters used by Chemburkar et al. (1987) ($\gamma \to \infty$, B, Da_1, ν, σ; see values in the caption for Figure 1) and two different values of the heat-transfer coefficient: $\alpha_T = 8.94$, which corresponds to a period-four (P_4) solution, and $\alpha_T = 9.0$, and which corresponds to the chaotic behavior in the corresponding CSTR. As expected, the homogeneous solutions become unstable at $Pe = Pe_0$ (Eq. 14). A further increase in Pe led to sequences of period-doubling bifurcations that yield the formation, in the limit $Pe \to \infty$, of the spatially oscillatory solutions of the same type as the corresponding CSTR problem [Figure 2 presents the bifurcation diagrams, calculated with the code AUTO (Doedel, 1981)].

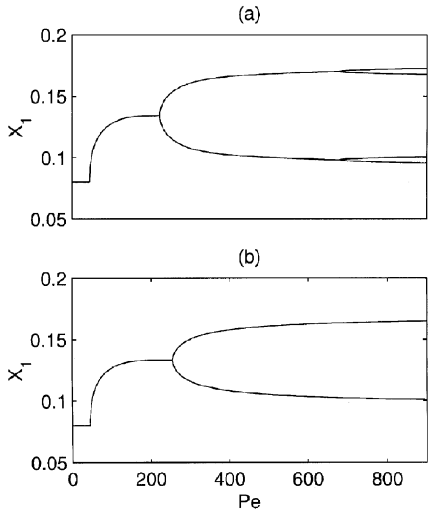

Figure 2. Bifurcation diagrams of Eq. 8 showing period-doubling transitions.

(a) Constant activity case, system convergences to a period-four solution; (b) varying activity case, $a_\phi = 100$, system convergences to a period-two solution. $\alpha_T = 8.94$ (other parameters as in Figure 1).

The varying catalytic activity case

Let us now allow for reversible changes in catalytic activity. In the limit of large Peclet numbers ($Pe \to \infty$), the steady-state solutions of the full system (Eqs. 4 and 7), are equivalent to the temporal solutions of the corresponding CSTR model with the modified kinetics

$$\frac{dx_1}{d\tau} = f(x_1, x_2, y, \phi), \qquad \frac{dx_2}{d\tau} = g(x_1, x_2, y, \phi)$$

$$\frac{dy}{d\tau} = h(x_1, x_2, y, \phi) \tag{15}$$

and

$$\phi = \frac{a_\phi - y}{b_\phi} \tag{16}$$

To simplify the following analysis, we used a_ϕ as a free parameter and defined $b_\phi = a_\phi - y_s$, in order to ensure $\phi_s = 1$, that is, the steady-state solution of the three-variable system (x_{1s}, x_{2s}, y_s) is also the solution of the full system with $\phi_s = 1$. Note that $\phi \to 1$ with $a_\phi \to \infty$.

The neutral curves (defined by $Re\sigma = 0$) for relatively large $a_\phi (> 100)$ preserved the same form as for the constant activity case and practically do not depend on the time scale, K_ϕ. For small a_ϕ the neutral curves changes drastically with increasing K_ϕ (see Figure 3). Note that the curves presented in Figure 3 are the projections of the 3-D curve $\mathfrak{D}(Pe, k, Im\sigma) = 0$ on the plane (Pe, k), and the loop observed in the Figure 3 corresponds to varying $Im\sigma$.

The critical parameters k_0, Pe_0 for the varying activity case can be determined by Eqs. 14 as well, using the gain differentiating rule for functions $f(x_1, x_2, y, \phi(y))$, $g(x_1, x_2, y, \phi(y))$ and $h(x_1, x_2, y, \phi(y))$, with $\phi(y)$ defined by Eq. 16. Typical

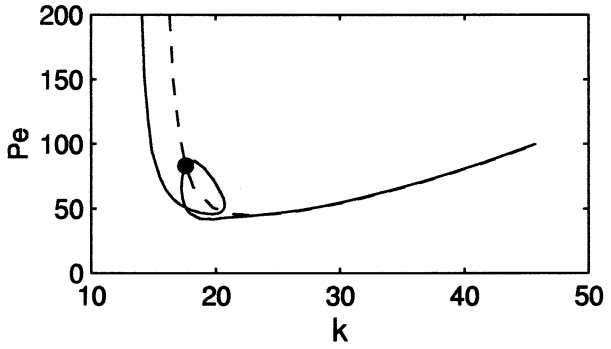

Figure 3. Varying activity case: effect of K_ϕ on neutral curves.

$K_\phi = 100$—solid line, 10,000—dashed line; $\alpha_T = 9$, $a_\phi = 10$, other parameters as in Figure 1.

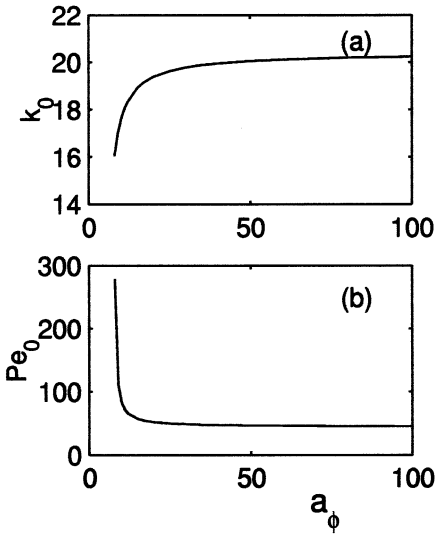

Figure 4. Varying activity case: effect of the coefficient a_ϕ on the critical parameters k_0 and Pe_0.

$\alpha_T = 8.94$; other parameters as in Figure 1.

dependencies of Pe_0, k_0 on a_ϕ are plotted in Figure 4. Obviously $\phi_s \to 1$ as $a_\phi \to \infty$, and the critical parameters tend to the asymptotic values corresponding to the three-variable system with fixed activity.

The amplitude bifurcation diagrams for very large a_ϕ preserve the same form as for the constant activity case. With decreasing a_ϕ the number of period doubling points for $Pe > Pe_0$ decreases. Thus, for $\alpha_T = 8.94$ the asymptotic behavior ($Pe \to \infty$) is a period-four (P_4) solution with $a_\phi = 1{,}000$ (as in the case $\phi = 1$), P_2 solution with $a_\phi = 100$ (see Figure 2b), while with $a_\phi = 10$ the single-loop oscillations are stable in the whole range $Pe_0 < Pe < \infty$. A similar tendency with decreasing a_ϕ was found for $\alpha_T = 9.0$, while for $a_\phi = 1{,}000$, we still find chaotic behavior; with $a_\phi = 100$, the sequence of bifurcations converges to a P_4, solution, and with $a_\phi = 10$, a period-one solution is stable for $Pe > Pe_0$ (Nekhamkina and Sheintuch, 2002).

Note that the stationary solutions predicted earlier for both regular and oscillatory kinetics need not necessarily be stable. A cross-flow reactor with a single chemical reaction exhibits a wide variety of spatiotemporal patterns, including standing and moving aperiodic waves (Nekhamkina et al., 2000b, 2001). Thus, numerical simulations are necessary to find the real solutions of the full distributed system (Eqs. 4, 5, 7).

Numerical Simulations

In this section we verify the analytical results presented in the previous chapter by direct numerical simulations of the distributed system (Eqs. 4 and 5). We verify the existence of stationary solutions and their bifurcations with increasing Pe, but we do not try to obtain the critical Pe values by numerical experiments, as it is a rather cumbersome problem.

As was shown in the previous studies (Andresén et al., 1999; Nekhamkina et al., 2000a), the boundary conditions applied at the inlet do not affect the regular periodic structure of stationary patterns sufficiently far from the reactor inlet, but rather define the length of the transition region. In order to diminish the inlet effect in simulations, we replaced the physically reasonable Danckwerts boundary condition with a simplified condition, $y = y_{in}$, and adjusted $x_{i,in}$, y_{in} to shorten the transition region. In all simulations we choose $Le = 100$ and set the reactor length $\tilde{L} = 10$.

Constant catalytic activity case

The expected stationary solutions were obtained in the whole range of Pe and α_T being considered. A typical sequence of period-doubling transitions of stationary spatially periodic solutions, for increasing Pe values, is shown in Figure 5. Below the critical Pe_0 (Eq. 14), the homogeneous solution is established practically in the whole reactor, with some adjustment in the inlet section (Figure 5a). Just above Pe_0, the system exhibits the stationary spatially periodic patterns. The regular single-loop structure is clearly seen in the "spatial" phase planes $x_1(\xi)$ vs. $x_2(\xi)$ (Figure 5 b(2); the entrance effect, $0 < \xi < 2.5$, is ignored). The computed wave numbers are in excellent agreement with the analytical predictions: the difference between the "numerical" and exact values k_0 is about 0.1%.

With increasing Pe the patterns transform in a way that follows the bifurcation diagram constructed in the previous section. Period-two solutions were obtained in the range $Pe_0 < Pe \simeq 700$ (Figure 5c), while for all $Pe > 700$, period-four

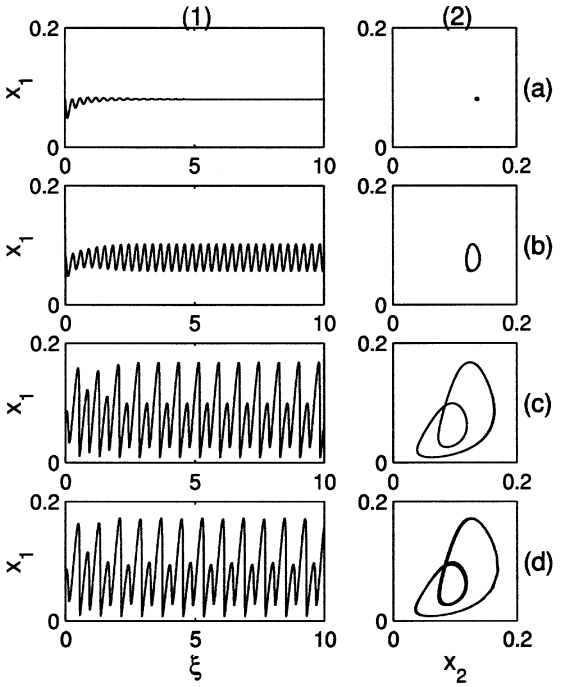

Figure 5. Bifurcation of spatial patterns [column (1)] in the constant activity case, calculated with $\alpha_T = 8.94$ for (row a) $Pe = 40 < Pe_0 = 44.03$, (b) $Pe = 50$, (c) 500, and (d) 1,000, and the corresponding "spatial" phase planes [column (2)], constructed from the data $2.5 < \xi < 10$).

Other parameters as in Figure 1.

Figure 6. Spatiotemporal gray-scale patterns of x_1 in the varying activity case.

$\alpha_T = 8.94$, $\alpha_\phi = 10$, $Pe = 500$, $K_\phi = 10^5$, $0 < \xi < 10$, $0 < \tau < 500$; other parameters as in Figure 1.

solutions (Figure 5d) were established. Note that the stationary solutions become practically insensitive to Pe for large $Pe(>10^3)$ and agree with the corresponding solutions of the mixed system with fixed initial conditions.

Obviously, by adjusting the parameters we can find more complex solutions of higher spatial periods. Yet, due to the finite size of the system, the exact pattern classification for high Pe is rather difficult. For this reason we cannot claim that the patterns will converge into a fully chaotic solution. These patterns can be called *stationary spatially aperiodic patterns*, and demonstration of such patterns is the main goal of the present investigation.

The varying catalytic activity case

The system behavior for sets of parameters that correspond to relatively small oscillations of the catalytic activity with $a_\phi = 100$ and moderate $K_\phi = 10^2 - 10^4$ is quite similar to the constant activity case: stationary patterns emerge above the critical $Pe = Pe_0$, and with increasing Pe, they bifurcate following the period doubling sequence.

The effect of decreasing a_ϕ or increasing K_ϕ is to destabilize the system by inducing a front motion, as in a typical activator–inhibitor system: ϕ is the slow variable and its response is more sluggish as K_ϕ increases. Beyond a certain threshold, the determination of which is beyond the scope of this study, the system undergoes a transition to spatiotemporal motion. Consider the case with $a_\phi = 10$, for which the analytical investigation predicts the formation of stationary spatially period-one patterns for all $Pe > Pe_0$ (for both $\alpha_T = 8.94$ and $\alpha_T = 9$). Numerical simulations reveal that these patterns are stable only for moderate Pe and K_ϕ values. A typical irregular pattern (Figure 6, simulated with $Pe = 500$, $\alpha_T = 8.94$, and $K_\phi = 10^5$) shows two domains and a fuzzy boundary: a regime of stationary standing waves exists upstream, while a domain of moving waves exists downstream. A section of a typical spatial profile (Figure 7a) shows that the wave numbers and the amplitudes of oscillations in the stationary ($\xi < 2.5$) and moving packages ($\xi > 2.5$) differ significantly. The power spectrum constructed from the data in the "fully developed" moving packages for $5 < \xi < 10$ (Figure 7b) allows us to distinguish several leading wave numbers ($k \sim 45$).

The irregular structure of the moving waves is clearly seen from the power spectrum of temporal signals at several fixed points. At $\xi = 2.5$, that is, around the boundary between the stationary and moving waves, we cannot discern any leading frequency (Figure 8a). The solution becomes more regular, but still incorporates many frequencies with increasing ξ (see the temporal profiles and the corresponding power spectrum for $\xi = 5$ and $\xi = 7.5$; Figures 8b and 8c).

Similar results of the formation of stationary spatially multiperiodic and complicated spatiotemporal patterns were obtained for $\alpha_T = 9$ (Nekhamkina and Sheintuch, 2002), but in comparison with the case $\alpha_T = 8.94$, the region where stable stationary spatially periodic patterns exist is shifted to a range of lower Pe and K_ϕ values. With increasing Pe or K_ϕ, the width of the stationary wave packet diminishes, while the moving packet broadens.

Concluding Remarks

Large-amplitude stationary spatially multiperiodic patterns have been simulated and analyzed in a cross-flow model with two consecutive reactions. These patterns emerge due to the interaction of reaction and convection of the state variables in a system with stationary boundary conditions applied at the inlet, in contrast to the Turing patterns that emerge due to competition of an activator and a diffusing inhibitor in quiescent fluids. The linear stability analysis for this model was performed using Pe as a bifurcation parameter, and an analytical expression for an amplification threshold was derived.

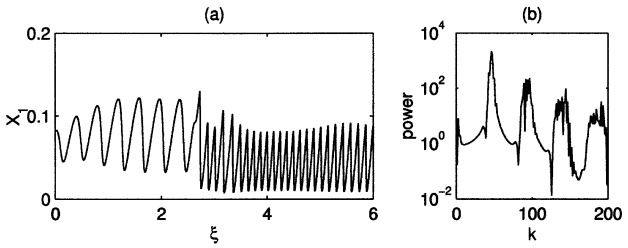

Figure 7. (a) Section of the $x_1(\xi)$ profile at a certain time and (b) power spectrum constructed from the data of the $x_1(\xi)$ profile in the interval $5 < \xi < 10$.

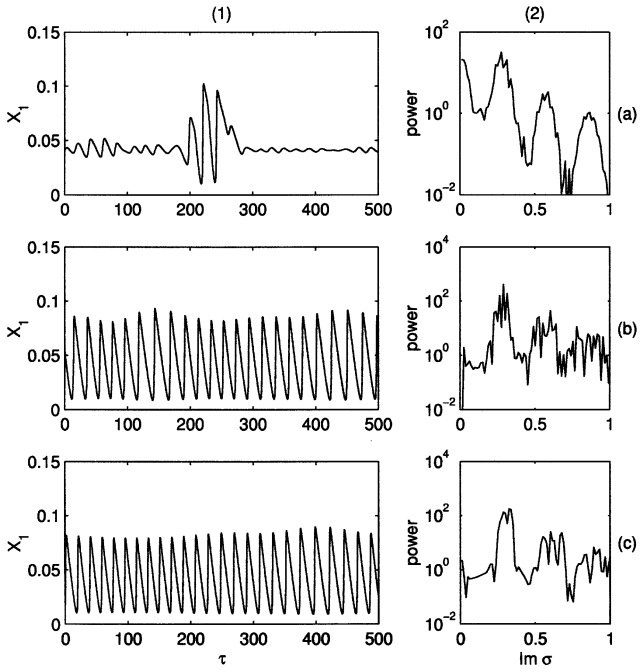

Figure 8. Temporal profiles of the concentration x_1 (column 1) and their power spectrum (column 2) at different cross sections: (a) $\xi = 2.5$, (b) $\xi = 5$, and (c) $\xi = 7.5$.

The following bifurcation analysis reveals a period doubling scenario that results in the formation of stationary spatially multiperiodic patterns, which in the limiting case $Pe \to \infty$ are identical to the temporal dynamics of a homogeneous CSTR with the same kinetics. Stationary patterns were simulated in the expected range of parameters, and the sequence of bifurcations and the critical parameters completely agree with the analytical predictions. With the oscillatory kinetics due to reversible catalytic activity, the stationary spatially chaotic patterns can become spatially and temporally chaotic (turbulent).

Note that the identification of the sustained patterns significantly depends on the reactor length, L. Obviously, it is impossible to observe spatially periodic patterns with a wavelength that is comparable with L. In the present study we observed up to period-four patterns for the regular kinetics case, and we can predict formation of more complicated structures with increasing L. On the other hand, the influence of the stationary boundary conditions applied at the inlet cannot propagate for an infinitely long distance. Thus, the behavior of a long system with complex patterns is still undetermined.

Acknowledgment

This work was supported by the Fund for Promotion of Research in the Technion and by U.S.-Israel Binational Science Foundation. One of the authors (O.N.) was supported in part by a Joint Grant from the Center for Absorption in Science of the Ministry of Immigrant Absorption and the Committee for Planning and Budgeting of the Council for Higher Education under the framework of the Camea Program. The other author (M.S.) is a member of the Minerva Center of Nonlinear Dynamics.

Literature Cited

Abashar, M. E., and S. S. E. H. Elnashaie, "Existence of Complex Attractors in Fluidized Bed Catalytic Reactors," *Chem. Eng. Commun.*, **158**, 1 (1997).

Andresén, P., M. Bache, E. Mosekilde, G. Dewel, and P. Borckmanns, "Stationary Space-Periodic Structures with Equal Diffusion Coefficients," *Phys. Rev. E*, **60**, 297 (1999).

Bamforth, J. R., S. Kalliadasis, J. H. Merkin, and S. K. Scott, "Modelling Flow-Distributed Oscillations in the CDIMA reaction," *Phys. Chem. Chem. Phys.*, **2**, 4013 (2000).

Bamforth, J. R., J. H. Merkin, S. K. Scott, R. Tóth, and V. Gáspár, "Flow-Distributed Oscillation Patterns in the Oregonator Model," *Phys. Chem. Chem. Phys.*, **3**, 1435 (2001).

Barto, M., and M. Sheintuch, "Excitable Waves and Spatiotemporal Patterns in a Fixed-Bed Reactor," *AIChE J.*, **40**, 120 (1994).

Berezowski, M., P. Ptaszek, and E. W. Jacobsen, "Dynamics of Heat-Integrated Pseudohomogeneous Tubular Reactors with Axial Dispersion," *Chem. Eng. Process.*, **39**, 181 (2000).

Chan, P. C.-H., D. G. Retzloff, R. Mohamed, and B. Berdouzi, "The Dynamic Behavior and Chaos for Two Parallel Reactions in a Continuous Stirred Tank Reactor," *Chem. Eng. Commun.*, **57**, 105 (1987).

Chemburkar, R. M., O. E. Rössler, and A. Varma, "Dynamics of Consecutive Reactions in a CSTR—A Case Study," *Chem. Eng. Sci.*, **42**, 1507 (1987).

De Wit, A., "Spatial Patterns and Spatiotemporal Dynamics in Chemical Systems," *Adv. Chem. Phys.*, **109**, 435 (1999).

Doedel, E. J., and R. F. Heinemann, "Numerical Computation of Periodic Solution Branches and Oscillatory Dynamics of the Stirred Tank Reactor with $A \to B \to C$ Reactions," *Chem. Eng. Sci.*, **38**, 1493 (1983).

Doedel, E. J., "AUTO, A Program for the Automatic Bifurcation Analysis of Autonomous System," *Congr. Numer.*, **30**, 265 (1981).

Frank-Kamenetski, D. A., *Diffusion and Heat Exchange in Chemical Kinetics*, Princeton Univ. Press, Princeton, NJ (1955).

Hua, H., M. Mangold, A. Kienle, and E. D. Gilles, "State Profile Estimation of an Autothermal Periodic Fixed-Bed Reactor," *Chem. Eng. Sci.*, **53**, 47 (1998).

Jorgensen, D. V., and R. Aris, "On the Dynamics of a Stirred Tank with Consecutive Reactions," *Chem. Eng. Sci.*, **38**, 45 (1983).

Jorgensen, D. V., W. W. Farr, and R. Aris, "More on the Dynamics of a Stirred Tank with Consecutive Reactions," *Chem. Eng. Sci.*, **39**, 1741 (1984).

Kuznetsov, S. P., E. Mosekilde, G. Dewel, and P. Borckmans, "Absolute and Convective Instabilities in a One-Dimensional Brusselator Flow Model," *J. Chem. Phys.*, **106**, 7609 (1997).

Lynch, D. T., "Chaotic Behavior of Reaction System: Mixed Cubic and Quadratic Autocatalysis," *Chem. Eng. Sci.*, **47**, 4435 (1992).

Lynch, D. T., T. D. Rogers, and S. E. Wanke, "Chaos in a Continuous Stirred Tank Reactor," *Math. Model.*, **3**, 103 (1982).

Merzhanov, A. G., and E. N. Rumanov, "Physics of Reaction Waves," *Rev. Mod. Phys.*, **71**, 1173 (1999).

Murray, J. D., *Mathematical and Biology*, Springer-Verlag, Berlin (1993).

Nekhamkina, O. A., A. A. Nepomnyashchy, B. Y. Rubinstein, and M. Sheintuch, "Nonlinear Analysis of Stationary Patterns in Convection-Reaction-Diffusion Systems," *Phys. Rev. E*, **61**, 2436 (2000a).

Nekhamkina, O. A., B. Y. Rubinstein, and M. Sheintuch, "Spatiotemporal Patterns in Thermokinetic Model of Cross-Flow Reactors," *AIChE J.*, **46**, 1632 (2000b).

Nekhamkina, O. A., B. Y. Rubinstein, and M. Sheintuch, "Spatiotemporal Patterns in Models of Cross-Flow Reactors. Regular and Oscillatory Kinetics," *Chem. Eng. Sci.*, **56**, 771 (2001).

Nekhamkina, O., and M. Sheintuch, "Spatially-'Chaotic' Solutions in Reaction-Convection Models and Their Bifurcations to Moving Waves," *Phys. Rev. E*, **66**, 016204 (2002).

Puszynski, J., D. Snita, V. Hlavacek, and H. Hoffman, "A Revision of Multiplicity and Parametric Sensitivity Concepts in Nonisothermal Nonadiabatic Packed Bed Chemical Reactors,"**36**, 1605 (1981).

Rovinsky, A. B., and M. Menzinger, "Chemically Instability Induced by a Differential Flow," *Phys. Rev. Lev.*, **69**, 1193 (1992).

Satnoianu, R. A., and M. Menzinger, "Non-Turing Stationary Patterns in Flow-Distributed Oscillators with General Diffusion and Flow Rates," *Phys. Rev. E*, **62**, 113 (2000).
Satnoianu, R. A., P. K. Maini, and M. Menzinger, "Parameter Space Analysis, Pattern Sensitivity and Model Comparison for Turing and Stationary Flow-Distributed Waves (FDS)," *Physica D*, **160**, 79, (2001).
Sheintuch, M., and O. Nekhamkina, "Pattern Formation in Homogeneous Reactor Models," *AIChE J.*, **45**, 398 (1999a).
Sheintuch, M., and O. Nekhamkina, "Pattern Formation in Homogeneous and Heterogeneous Reactor Models," *Chem. Eng. Sci.*, **54**, 4535 (1999b).
Sheintuch, M., and S. Shvartsman, "Spatiotemporal Patterns in Catalytic Reactors," *AIChE J.*, **42**, 1041 (1996).
Turing, A. M., "The Chemical Basis for Morphogenesis," *Philos. Trans. R. Soc. B*, **237**, 37 (1952).
Yakhnin, V. Z., A. B. Rovinsky, and M. Menzinger, "Differential Flow Instability of the Exothermic Standard Reaction in a Tubular Cross-Flow Reactor," *Chem. Eng. Sci.*, **49**, 3257 (1994).
Zeldovich, J. B., and G. I. Barenblatt, "Theory of Flame Propagation," *Combust. Flame*, **3**, 61 (1959).

Manuscript received May 21, 2002, and revision received Sept. 30, 2002.